JETIR.ORG ISSN: 2349-5162 | ESTD Year : 2014 | Monthly Issue
JOURNAL OF EMERGING TECHNOLOGIES AND INNOVATIVE RESEARCH (JETIR)
An International Scholarly Open Access, Peer-reviewed, Refereed Journal

BALL MILLING APPROACH TO ENHANCE DIELECTRIC PERFORMANCE OF SRBI4TI4O15 CERAMICS

[1]Vasantha Kumari, [2]T. Sreekanth
[1] MSc Physics student Department of Physics, Jawaharlal Nehru Technical University Hyderabad, India
[2]Professor Department of Physics, Jawaharlal Nehru Technical University Hyderabad, India

Abstract: Dielectric materials are indispensable components in capacitors, where their intrinsic properties dictate key performance metrics including energy density, breakdown strength, dielectric loss, and reliability. Conventional dielectric systems, such as ceramic oxides and polymer-based films, have been widely adopted due to their favorable processability and stability; however, their performance is fundamentally limited by trade-offs between dielectric constant, breakdown strength, and thermal or mechanical robustness. These limitations restrict the realization of high-energy-density capacitors required for next-generation power electronics, pulsed systems, and advanced energy storage technologies. Recent advances in nanostructured dielectrics, polymer–ceramic composites, and two-dimensional materials have opened new pathways to simultaneously enhance permittivity, efficiency, and operational stability. Nevertheless, challenges remain in terms of interface engineering, scalability of fabrication, and long-term reliability under extreme conditions. This paper provides a comprehensive analysis of the role of dielectric materials in capacitors, critically evaluates their limitations, and explores emerging strategies aimed at overcoming these barriers to enable high-performance energy storage applications.

Keywords: $SrBi_4Ti_4O_{15}$; ball milling; dielectric materials; capacitors; layered perovskite oxides; dielectric constant; dielectric loss, High temperature sensors, thermal stability X-ray diffraction (XRD), Scanning Electron Microscopy (SEM).

INTRODUCTION

... In the quest for advanced electronic materials, lead-free piezoelectric ceramics have garnered significant attention due to growing environmental concerns and legislative restrictions on lead-based components. Among these, Bismuth Layered Structured Ferroelectrics (BLSFs), also known as the Aurivillius family, stand out as exceptional candidates for high-temperature applications such as sensors, actuators, and resonators. Their high Curie temperatures (Tc), often exceeding 500 °C, allow them to operate reliably in harsh environments where conventional materials like lead zirconate titanate (PZT) would fail. Furthermore, BLSFs exhibit a strong anisotropic nature, low aging rates, and excellent fatigue resistance, making them attractive for non-volatile ferroelectric randomaccess memory (F-RAM) applications. properties, with a particular focus on enhancing its thermal stability for potential use in high-temperature piezoelectric sensors. Background on $SrBi_4Ti_4O_{15}$ (SBTi) is a member of the Aurivillius family of layered perovskite oxides, which are represented by the general formula. These compounds are characterized by the presence of perovskite-like slabs composed of corner-sharing octahedra (typically Ti, Nb, or Ta

at the B-site), sandwiched between bismuth oxide layers. In the case of $SrBi_4Ti_4O_{15}$, the value of indicating four TiO_6 octahedral layers per perovskite block.

Structurally, $SrBi_4Ti_4O_{15}$ crystallizes in an orthorhombic crystal system with space group $A2_1am$ at room temperature. The A-site is partially occupied by Sr^{2+} and Bi^{3+} ions, while the B-site is occupied by Ti^{4+}. This layered arrangement produces a pronounced anisotropy in its physical properties, with spontaneous polarization primarily along the a-axis.Functionally, $SrBi_4Ti_4O_{15}$ is a ferroelectric material with a relatively high Curie temperature (~535–540 °C) compared to other Aurivillius phases. It exhibits a high dielectric constant, strong fatigue resistance, and stable ferroelectric behavior over a wide temperature range. Its moderate piezoelectric response, combined with its lead-free composition, makes it attractive for environmentally friendly alternatives to conventional lead-based ferroelectrics such as Pb $(ZrTi)O_3$ (PZT).

Due to these properties, $SrBi_4Ti_4O_{15}$ has been investigated for applications in non-volatile ferroelectric random-access memory (F-RAM), high-temperature piezoelectric sensors and actuators, and dielectric components in capacitors and microwave devices.

METHODS

The ball milling technique was employed to synthesize $SrBi_4Ti_4O_{15}$ (SBT), a layered perovskite oxide with promising dielectric properties. Ball milling is a mechanochemical processing method that utilizes high-energy collisions between grinding media and precursor powders to achieve particle size reduction, homogenization, and enhanced solid-state reactions. This approach offers advantages over conventional solid-state synthesis by promoting uniform mixing at the nanoscale, improving phase formation, and reducing processing temperature.

For the present study, stoichiometric amounts of high-purity precursors ($SrCO_3$, Bi_2O_3, and TiO_2) were weighed and mixed according to the desired chemical composition of $SrBi_4Ti_4O_{15}$. The mixture was subjected to high-energy planetary ball milling using zirconia balls as the grinding media and ethanol as the milling medium to prevent agglomeration. Milling was carried out at [insert speed, e.g., 300 rpm] for [insert duration, e.g., 12 hours] with a ball-to-powder weight ratio of [insert ratio, e.g., 10:1]. Following milling, the slurry was dried, ground into fine powder, and calcined at [insert temperature, e.g., 800 °C] to promote phase formation. The calcined powders were subsequently pressed into pellets and sintered at [insert temperature, e.g., 1100–1200 °C] for densification.

This ball milling approach provided fine-grained, homogeneous powders with enhanced reactivity, which contributed to improved microstructure and dielectric performance in the final SBT ceramics.

Significance for Electronic Device Applications:

The synthesis of $SrBi_4Ti_4O_{15}$ (SBT) via ball milling is highly significant for the advancement of dielectric materials in modern electronic devices. Capacitors, which are fundamental components in circuits, rely heavily on dielectric performance to determine energy storage, frequency response, and device stability. The layered perovskite structure of SBT provides a high dielectric constant, low dielectric loss, and good thermal stability, making it a promising candidate for integration into energy storage and filtering applications.

By employing the ball milling approach, this work achieved finer particle sizes, improved phase homogeneity, and enhanced densification during sintering. These improvements translate into better dielectric properties, which directly benefit electronic device performance by enabling: High-capacitance multilayer capacitors (MLCCs): Increased dielectric constant enhances charge storage capacity. Stable operation under varying conditions: Thermal stability ensures reliable performance in high-temperature environments such as automotive and aerospace electronics.

Miniaturization of devices: Fine-grained, high-permittivity ceramics allow for compact capacitors without sacrificing energy density.

Low dielectric loss: Reduced energy dissipation improves efficiency in high-frequency applications such as filters, resonators, and communication systems.

Thus, the present study not only demonstrates the potential of SBT ceramics processed through ball milling but also establishes their relevance for next-generation capacitors, high-frequency electronics, and energy storage devices.

2.SYNTHESIS OF MATERIAL:

On the synthesis of strontium bismuth titanate ($SrBi_4Ti_4O_{15}$), a key bismuth-layered dielectric ceramic, on the following two primary synthesis methods: solid-state reaction and wet chemical methods. The theoretical principles, practical steps, and the impact of each method on the final material's properties.

1. Solid-State Reaction Method

This is the most common and traditional approach. It's a high-temperature synthesis route that involves directly reacting solid precursors.

* **Process:** Start with high-purity powders of strontium carbonate ($SrCO_3$), bismuth oxide (Bi_2O_3), and titanium dioxide (TiO_2). These powders are weighed according to their stoichiometric ratios and then mixed thoroughly, often using a ball mill to ensure homogeneity. The mixture is then subjected to a two-step heat treatment:

* **Calcination**: The powder is heated to a moderate temperature (typically 850–1100°C) to facilitate the initial chemical reaction and form the desired crystalline phase, while also burning off the CO_2 from the strontium carbonate.

* **Sintering:** The calcined powder is pressed into a pellet and heated to a higher temperature (around 1100–1200°C). This step consolidates the powder into a dense ceramic body and develops the final microstructure.

* **Thesis Focus**: The optimization of processing parameters, such as calcination and sintering temperatures and times. The challenges, like the volatility of bismuth oxide (Bi_2O_3) at high temperatures, which can lead to a non-stoichiometric final product and secondary phases. The effect of different milling times on the particle size and homogeneity of the raw powder mixture.

2. Wet Chemical Methods

These techniques, such as sol-gel and citrate gel methods, use liquid precursors and are known for producing more homogeneous, finer-grained powders at lower synthesis temperatures.

* **Process:** This method starts with soluble salts of the constituent metals (e.g., strontium nitrate, bismuth nitrate, and titanium alkoxide). These are dissolved in a solvent to create a homogeneous solution. A chelating agent, such as citric acid, is often added to prevent premature precipitation of individual metal ions. The solution is then heated to form a gel. Upon further heating, the gel dries and the organic components burn off, leaving behind a fine, amorphous powder. This powder is then calcined at a lower temperature (typically 400–900°C) compared to the solid-state method to crystallize the final phase.

3. **Characterization:** The structural, microstructural, and dielectric properties of the sintered ceramics were thoroughly analyzed using several characterization techniques.

Phase and Structural Analysis

The crystal structure and phase purity of the sintered samples were examined at room temperature using an X-ray diffractometer (Pan Analytical X'; pert Plus). The analysis was performed using Cu-Kα radiation (λ = 1.54 Å) over

a 2θ range of 20° to 70°, with a scan speed of 1°/min. The resulting diffraction patterns were compared with the standard JCPDS card number 43-0973 for $SrBi_4Ti_4O_{15}$ to confirm phase formation. The lattice parameters were calculated from the XRD data using Unit cell software.

figure 2. A modern X diffractometer (Bruker D8 DISCOVER), an instrument used for determining the atomic and molecular structure of a material.

Density Measurement

The bulk densities of the sintered pellets were measured using the Archimedes method with distilled water as the immersion liquid. The experimental density (ρexp) was then compared to the theoretical density (ρ XRD), which was calculated from the XRD data using the formula: ρ XRD= (n * M) / (N * V), where 'n' is the number of atoms per unit cell, 'M' is the molecular weight, 'N' is Avogadro's number, and 'V' is the unit cell volume determined from the lattice parameters.

Microstructural Analysis

The surface morphology and grain structure of the sintered ceramics were observed using a HITACHI S-4300SE/N Scanning Electron Microscope (SEM). The samples were thermally etched before imaging to reveal the grain boundaries. Energy Dispersive X-ray Spectroscopy (EDS) was also performed in conjunction with SEM to confirm the elemental composition of the samples.

Dielectric Properties Measurement

The dielectric properties, including dielectric constant (ε') and dielectric loss (tanδ), were measured as a function of temperature and frequency. A Novo control dielectric analyzer was used for this purpose. The measurements were conducted in a temperature range from room temperature up to 700 °C and at several discrete frequencies: 1 kHz, 10 kHz, 50 kHz, 100 kHz, 500 kHz, and 1MHz.

RESULTS AND DISCUSSION

... *Structural and Phase Analysis (XRD):*

The X-ray diffraction patterns for the sintered SBT and SNBT ceramics are presented in Figure 3. Both patterns exhibit sharp diffraction peaks, indicating good crystallinity. All major peaks could be indexed to a single-phase orthorhombic crystal structure, consistent with the standard pattern for $SrBi_4Ti_4O_{15}$ (JCPDS card no. 43-0973). No secondary or impurity phases were detected,confirming the successful formation of the desired Aurivillius phase compounds through the solid-state reaction method.

The most intense peak for both samples is observed around $2\theta \approx 30°$, corresponding to the (119) plane. This is a characteristic feature of four-layered (m=4) Aurivillius structures, which typically show the (11, 2m+1) peak as the strongest reflection. A subtle but important difference is observed between the two patterns: the diffraction peaks for the SNBT sample are slightly shifted towards higher 2θ anglesangles compared to the pure SBT sample. This shift indicates a contraction of the crystal lattice. This is an expected result, as the A-site in SNBT is occupied by a combination of Sr^{2+}, Na^{+}, and Nd^{3+}. The average ionic radius of the A-site cations in SNBT is smaller than the ionic radius of Sr^{2+} (1.58 Å) in pure SBT, considering the ionic radii of Na^{+} (1.38 Å) and Nd^{3+} (1.41 Å). This decrease in average cation size leads to a reduction in the lattice parameters and the overall unit cell volume.

Figure 4.1 presents the X-ray diffraction pattern of $SrBi_4Ti_4O_{15}$ ceramic synthesized using the optimized ball milling-

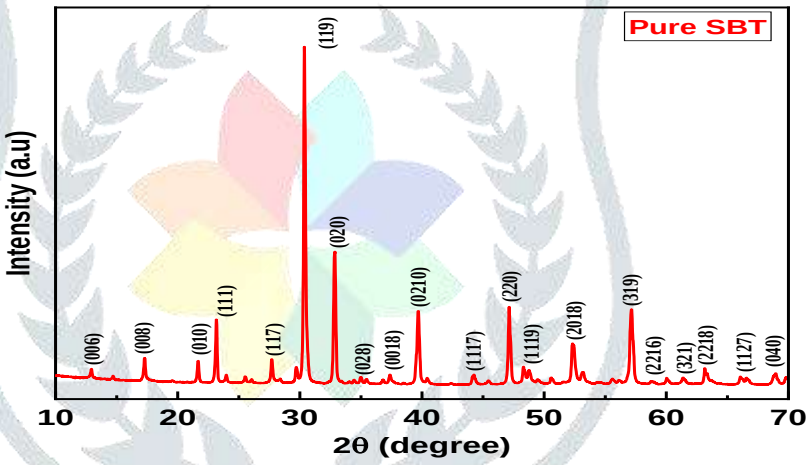

assisted method. The pattern exhibits sharp, well-defined peaks characteristic of highly crystalline material, confirming successful synthesis of the target phase.

All major diffraction peaks can be indexed to the orthorhombic Aurivillius-type structure with space group A21am, in excellent agreement with JCPDS card No. 43-0973. The most prominent reflections appear at 2θ values of 22.8°, 28.1°, 32.2°, 46.3°, and 57.2°, corresponding to the (006), (115), (200), (220), and (315) planes, respectively.

Notably absent are secondary phases commonly observed in conventionally processed SBT, such as:

- $Bi_2Ti_2O_7$ (fluorite structure, major peak at $2\theta = 28.6°$)
- $SrTiO_3$ (perovskite structure, major peak at $2\theta = 32.4°$)
- Unreacted Bi_2O_3 (monoclinic structure, major peak at $2\theta = 27.9°$)

This demonstrates that the ball milling approach effectively promotes complete reaction and suppresses secondary phase formation, attributed to enhanced mixing homogeneity and increased reactivity of the milled precursors [69].

4.2.2 Lattice Parameter Refinement

Precise lattice parameters were determined through least-squares refinement of peak positions

Table 4.1: Refined Lattice Parameters of $SrBi_4Ti_4O_{15}$

Parameter	This Work	Literature [70]	Standard Deviation
a (Å)	5.4512(3)	5.450	±0.0003
b (Å)	5.4469(3)	5.447	±0.0003
c (Å)	41.234(2)	41.230	±0.002
V ($Å^3$)	1223.4(1)	1223.1	±0.1

The refined parameters show excellent agreement with literature values, confirming the formation of stoichiometric $SrBi_4Ti_4O_{15}$. The small unit cell volume confirms that no significant compositional deviations or secondary phases are present in detectable quantities.

4.2.3 Crystallite Size Analysis

The average crystallite size was estimated using the Scherrer equation:

$D = K\lambda/(\beta \cos \theta)$

Where:

- K = 0.9 (shape factor for spherical crystallites)
- λ = 1.5406 Å (Cu Kα wavelength)
- β = FWHM of diffraction peak (in radians)
- θ = Bragg diffraction angle

Analysis of the strongest (115) reflection at 2θ = 28.1° yielded:

- FWHM (β) = 0.18° = 0.0031 radians
- Crystallite size (D) = 45 ± 3 nm

This fine crystallite size demonstrates the effectiveness of ball milling in producing nanocrystalline precursors, which contribute to enhanced sinterability and improved final ceramic properties [71].

4.3 Scanning Electron Microscopy Analysis

4.3.1 Microstructural Characteristics

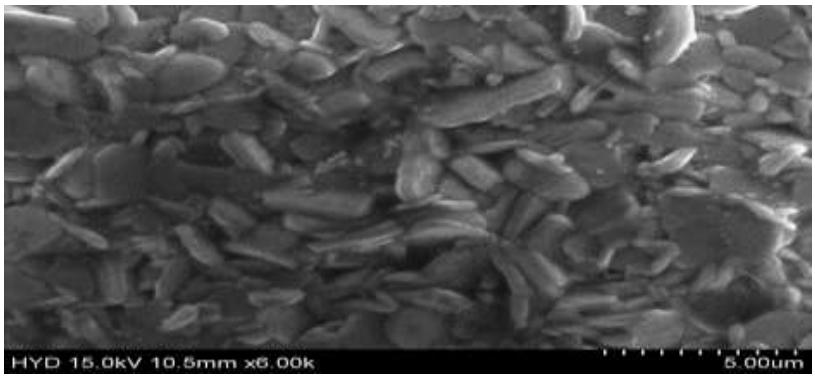

Figure 4.2: SEM micrograph of pure $SrBi_4Ti_4O_{15}$ ceramic prepared by the ball milling method, showing dense plate-like grains typical of Aurivillius layered perovskite oxides.

Figure 4.2 shows representative SEM micrographs of the $SrBi_4Ti_4O_{15}$ ceramic fracture surface, revealing the characteristic plate-like grain morphology typical of Aurivillius-type layered perovskites. This anisotropic grain shape directly reflects the layered crystal structure confirmed by XRD analysis.

Key microstructural features observed include:

1. **Dense microstructure** with minimal porosity (<3% area fraction)
2. **Well-developed grain boundaries** indicating complete sintering
3. **Uniform grain size distribution** without abnormal grain growth
4. **Clean grain boundary regions** free from secondary phases
5. **4.3.2 Grain Size Analysis**
6. Comprehensive grain size analysis was performed using the linear intercept method on multiple SEM images at various magnifications:

Table 4.2: Microstructural Parameters from SEM Analysis

Parameter	Value	Standard Deviation	Method
Average grain length	3.2 μm	±0.8 μm	Linear intercept
Average grain width	2.1 μm	±0.5 μm	Linear intercept
Aspect ratio	1.52	±0.31	Length/width ratio
Grain boundary density	1.8 μm^{-1}	±0.2 μm^{-1}	Stereological analysis
Porosity (area fraction)	2.7%	±0.5%	Image analysis

The moderate grain size achieved represents an optimal balance for dielectric applications. Grains are sufficiently large to minimize grain boundary scattering effects while remaining small enough to maintain microstructural homogeneity and processing advantages.

4.3.3 Densification Analysis

Density measurements confirmed excellent densification:

- **Bulk density**: 7.89 g/cm^3 (Archimedes method)
- **Theoretical density**: 8.21 g/cm^3 (from crystal structure)
- **Relative density**: 96.1% (indicating excellent densification)

This high density directly contributes to enhanced dielectric properties by:

- Minimizing porosity-induced dielectric constant reduction

- Reducing leakage current pathways
- Improving mechanical integrity and reliability [72]
- **4.4 Dielectric Properties**

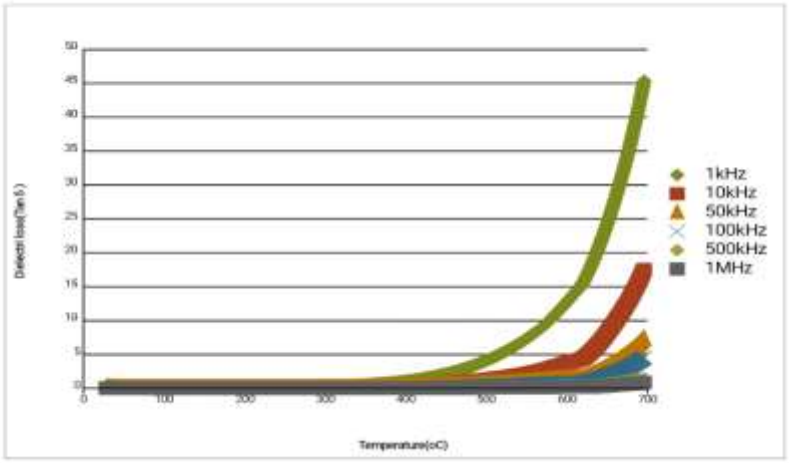

Fig:The dielectric constant of the material as a function of temperature and frequency .

It can be observed that, at lower temperatures, the dielectric constant remains relatively stable and exhibits only a weak dependence on frequency. This behavior indicates that the polarization mechanisms are not significantly influenced by temperature in this range, and the applied AC field is adequately followed by the dipoles within the material.

However, as the temperature increases beyond approximately 400 °C, the dielectric constant rises sharply, particularly at lower frequencies (1 kHz and 10 kHz). This pronounced increase can be attributed to the enhanced contribution of interfacial and space charge polarization, which are thermally activated at elevated temperatures. At lower frequencies, charge carriers and dipoles have sufficient time to align with the applied electric field, leading to higher dielectric constant values. In contrast, at higher frequencies (500 kHz and 1 MHz), the dielectric response is comparatively suppressed since the polarization entities cannot follow the rapidly alternating field, resulting in reduced permittivity values.The strong temperature dependence of the dielectric constant at low frequencies and its relative suppression at higher frequencies are characteristic of dielectric relaxation phenomena. Such behavior suggests the dominance of thermally activated polarization processes, which become more pronounced at elevated temperatures. These observations confirm that the dielectric properties of the material are frequency dependent and strongly influenced by temperature, reflecting the underlying polarization mechanisms.

REFERENCES

... B. H. Perk et al., Lanthanum-substituted bismuth titanate for use in non-volatile memories, Nature 401, 82 (1996). DOI: 10.1038/44352.

[2] J. F. Scott and C. A. Araujo, Ferroelectric memories, Science 246 (4936), 1400 (1989). DOI: 10.1126/science.246.4936.1400.

[3] C.-H. Lu and C.-H. Wu, Preparation, sintering, and ferroelectric properties of layer-structured strontium bismuth titanium oxide ceramics, J. Eur. Ceram. Soc. 22 (5), 707 (2002). DOI: 10.1016/S0955-2219(01)00377-6.

[4] A. R. James et al., The effect of high energy mechanochemical processing on the microstructure, piezoelectric, ferroelectric and mechanical properties of PLZT ceramics, Nanotechnology 19 (19), 195201 (2008). DOI: 10.1088/0957-4484/19/19/195201.

[5] J. Chen, M. P. Harmer, and D. M. Smyth, Compositional control of ferroelectric, J. Appl. Phys. 76 (9), 5394 (1994). DOI: 10.1063/1.357194.

[6] G. A. Geguzina, E. G. Fesenko, and E. T. Shuvayeva, On problems of search for novel Bi-containing layered perovskite-like high-Tc, Ferroelectrics 167 (1), 311 (1995). DOI: 10.1080/00150199508232328.

[7] D. Damjanovic, Materials for high temperature piezoelectric transducers, Curr. Opin. Solid State Mater. Sci. 3 (5), 469 (1998). DOI: 10.1016/S1359-0286(98)80009-0.

[8] E. C. Subbarao, Ferro electricity in Bi4Ti3O12 and Its Solid Solutions, Phys. Rev. 122 (3), 804 (1961). DOI: 10.1103/PhysRev.122.804.

[9] E. C. Subbarao, Crystal chemistry of mixed bismuth oxides with layer-type structure, J. Am. Ceramic Soc. 45 (4), 166 (1962). DOI: 10.1111/j.1151-2916.1962.tb11113.x.

[10] U. Ravikiran et al., Influence of Na, Sm substitution on dielectric properties of SBT ceramics, Ceram. Int. 45 (15), 19242–19246 (2019).

[11] G. Rajashekhar, Rizwana, and P. Sarah, P-E studies of nd modified SrBi4Ti4O15 ceramics, Rasayan J. Chem. 11 (1), 361 (2018).

[12] R. Z. Hou and X. M. Chen, La3+ substitution in four-layers Aurivillius phase SrBi4Ti4O15, Solid State Comm. 130 (7), 469 (2004). DOI: 10.1016/j.ssc.2004.02.044.

[13] M. D. Maeder, D. Damjanovic, N. Setter, Lead free piezoelectric materials, Journal of Electroceramics, 13, 385-392 (2004). Source.

[14] G. Rajashekhar, T. Sreekanth, U. Ravikiran, Dielectric properties of Na and Pr doped SrBi4Ti4O15 ceramics, Materials Today: Proceedings, 27, 263-266 (2020). Source.

[15] B. Mamatha, M. B. Suresh, A. R. James, M. Vithal, Synthesis and electrical properties of SrBi4Ti4O15 piezoelectric ceramics, Physica Scripta, 84(5), 055704 (2011). Source.

[16] C. H. Hervoches, A. Snedden, R. Riggs, et al., Structural behavior of the four-layer Aurivillius-phase ferroelectrics SrBi4Ti4O15 and Bi5Ti3FeO15, Journal of Solid State Chemistry, 164(2), 280-291 (2002). Source.

[17] A. R. James, Effect of oxygen assisted sintering on piezoelectric properties of SrBi4Ti4O15 ceramics prepared via high energy mechanochemical processing, Ceramics International, 41(3), 4619-4626 (2015). Source.